A Dual-Field Inertial–Acoustic Microfluidic Chip for Label-Free Circulating Tumor Cell Isolation

Feiqi (Carl) Chen, Culver Academies, Indiana, USA

Background & Significance

Circulating Tumor Cells

- Circulating tumor cells (CTCs) are extremely rare cancer cells from primary tumors into the bloodstream and serve as important biomarkers for early cancer detection, prognosis prediction, and treatment monitoring.
- CTCs occur at extremely low concentrations-often fewer than 10 cells per milliliter of blood-making their isolation technically challenging.

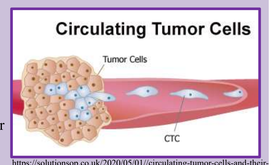

https://solutionsop.co.uk/2020/05/01//circulating-tumor-cells-and-their-future-in-oncology-diagnostic

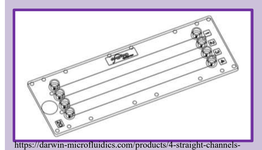
https://darwin-microfluidics.com/products/4-straight-channels-chip-miniluer?srsltid=AfmBOoo0J8gnUGh2ZTjxIP-M1j0Z9-8AB0PBBWHhlkU5pvJhxkCRAxyv

- Microfluidic chips are devices that manipulate small volumes of fluids within microscale channels.
- Fluid flow is highly controlled and predictable, enabling precise handling of cells and particles.

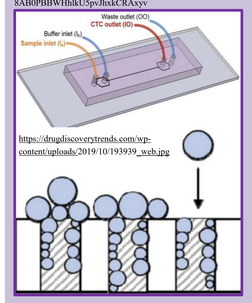

https://drugdiscoverytrends.com/wp-content/uploads/2019/10/193939_web.jpg

Label-Based Capture

- Uses antibodies or magnetic particles to bind CTCs
- Marker variability leads to incomplete capture

Size-Based Filtration

- Separates cells using membranes or microstructures
- Prone to clogging during continuous operation

Single-Field Microfluidic Separation

- Manipulates cells using a single physical force
- Tradeoffs between efficiency, purity, and stability

Clinical and Practical Limitations:

- ☐ CellSearch® - only FDA-approved CTC detection system.
- ☐ **EpCAM-based** immunomagnetic capture
- ☐ During **epithelial–mesenchymal transition (EMT)**, CTCs may **lose EpCAM expression**

Region/Provider	Cost (approx.)	Notes
United States	~ $ 2,689	Includes professional interpretation in billing data (Towards Healthcare)
Bangkok	~ $ 1,450	Local private clinic pricing example (SC21 Medical Centra Bangkok)
Hong Kong	~ $ 1,280-2560	Local range reported by provider (cancer.lifeclinic.com.hk)
China	~ $ 500	Local range reported by provider

Engineering Goal

Limitations of Conventional Microfluidic Approaches:


https://darwin-microfluidics.com/products/4-straight-channels-chip-miniluer?srsltid=AfmBOoo0J8gnUGh2ZTjxIP-M1j0Z9-8AB0PBBWHhlkU5pvJhxkCRAxyv

- ☐ Single-field separation limits efficiency and accuracy under high throughput
- ☐ Particle–wall interactions cause adhesion and fouling
- ☐ Reduced stability during continuous operation

Engineering Objectives:

Goal 1: Dual-Field, Label-Free Separation

- ✓ Inertial focusing + acoustic manipulation
- ✓ >95% particle separation efficiency
- ✓ >3 X throughput

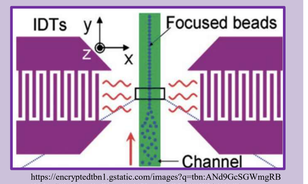

https://encrypted-tbn1.gstatic.com/images?q=tbn:ANd9GcSGWmgRBZ4iNaf0UlyVwKaQNm49cU51b_UKQ54I80CD6KX-Tj

Goal 2: Anti-Adhesion and Operational Stability

- ✓ Micropillar anti-adhesive surfaces
- ✓ Chemical surface modification
- ✓ 72 h continuous operation

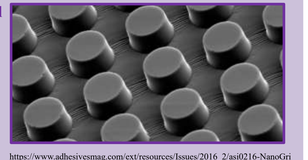
https://www.adhesivesmag.com/ext/resources/Issues/2016_2/asi0216-NanoGrip-Fig 1-microfiber.webp

Engineering Question:

Can a microfluidic chip be engineered to achieve high-efficiency, label-free particle separation while maintaining stable, low-adhesion operation under continuous flow conditions?

Principle Overview

Inertial separation

- Inertial lift + Dean flow focus particles into size-dependent equilibrium positions.
- Provides high-throughput pre-focusing to simplify downstream separation.
- Inertial pre-alignment reduces dispersion, improving acoustic selectivity and outlet purity.

Acoustic separation

- Acoustophoresis applies an acoustic radiation force that scales strongly with particle size ($\propto a^3$).
- Enables gentle, contactless lateral migration for fine separation after pre-focusing.
- Sequential fields aim to reduce the efficiency-throughput tradeoff of single-field methods.

Anti-adhesion strategy

- SiO_2 micropillar textures reduce particle–wall contact and stagnation zones.
- Chemical surface modification is planned to suppress nonspecific adhesion for long-term operation.

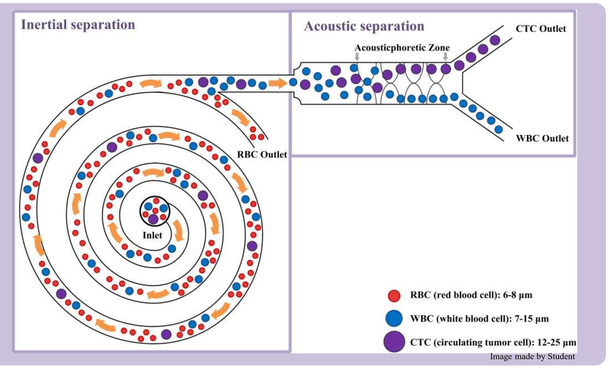

Image made by Student

Methodology and Design Specifics

Chip Structural Design

Upstream Inertial Spiral Module

- Geometry: 20 mm diameter spiral | 3.3 turns | 1.5 mm pitch
- Channel cross-section: 200 × 100 μm
- Size-dependent lift forces drive larger CTC analogs toward distinct equilibrium streamlines
- Smaller RBC analogs remain closer to inner streamlines
- High-throughput and passive pre-alignment

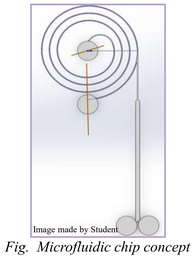
Image made by Student
Fig. Microfluidic chip concept

Downstream Acoustic Separation Channel

- Channel dimensions: 800 × 100 μm
- Active length: 25 mm
- A bonded piezoelectric transducer generates a standing acoustic wave across the channel width
- Acoustic radiation forces scale with particle volume, enabling differential migration
- Larger CTC analogs migrate toward pressure nodes more rapidly than WBC analogs

Image made by Student
Fig. Microfluidic chip prototype

Inertial Separation in the Spiral Microchannel:

- Within the spiral microchannel, particles experience inertial lift forces and curvature-induced Dean flow.
- Flow operates at a moderate Reynolds number, maintaining laminar conditions while enabling inertial effects (1)
- Particles experience inertial lift forces and Dean drag, leading to size-dependent equilibrium focusing.
- The inertial lift force scales as (2)
- Larger WBC & CTC analogs migrate to lateral positions compared to smaller RBC analogs.

$$\mathrm{Re} = \frac{\rho U D_h}{\mu} \quad (1) \qquad F_L \propto \rho U^2 a^4 / D_h^2 \quad (2)$$

Acoustic Separation in the Straight Channel:

- Acoustic separation is implemented using a piezoelectric transducer (PZT) bonded to the exterior of the microfluidic chip adjacent to the straight separation channel.
- The PZT converts electrical energy into mechanical vibrations, generating a standing acoustic wave across the channel width.
- At resonance, pressure nodes and antinodes form, inducing acoustic radiation forces on suspended particles (3)
- This strong size dependence enables refined, label-free separation following inertial pre-alignment.

$$F_{rad} \propto a^3 \nabla E a c \quad (3)$$

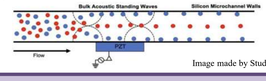

Image made by Student

Anti-Adhesion Design

Microscale SiO_2 micropillar arrays along channel walls reduce stable particle-wall contact by:

- decreasing effective contact area
- maintaining elevated near-wall shear
- suppressing low-velocity stagnation zones

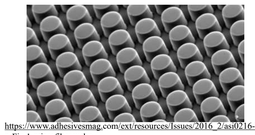
https://www.adhesivesmag.com/ext/resources/Issues/2016_2/asi0216-NanoGrip-Fig 1-microfiber.webp

Antifouling Surface Chemistry

PEG-based coatings

- Hydrophilic polymer coatings
- Reduce nonspecific adsorption via steric
- epulsion + hydration
- Simpler to implement on PDMS/glass

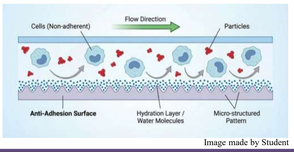

Image made by Student

Experimental Setup

COMSOL Simulation

- Laminar Flow + Particle Tracing
- Geometry matches fabricated chip Particle sizes: 20 μm (CTC), 10 μm (WBC), 6–7 μm (RBC)
- Material: polystyrene, ρ = 1050 kg/m³
- Wall interaction: bounce model enabled
- Laminar flow maintained throughout device

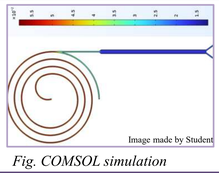
Image made by Student
Fig. COMSOL simulation

Microfluidic Experiments

- Syringe pump-driven flow through PDMS chip
- Working fluid: De-ionized water
- Test particles: 2, 7, 10, 20 μm fluorescent microspheres
- Flow rates: 0.8-2.5 mL/h
- Optimal separation at: ~1.5-2.0 mL/h
- Monitor device: PC + high-resolution experimental camera

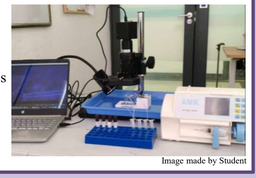
Image made by Student

Acoustic Channel Testing System Design

- Custom acoustic platform for standing-wave generation
- 16 mm PZT transducer (13.8–140 kHz), frequency-tunable
- Adjustable 3D-printed alignment stage
- Water immersion for impedance matching
- Controlled laminar flow (0.8–2.5 mL/h)
- Frequency sweep to identify resonance
- Particle focusing used to verify standing-wave formation
- Real-time imaging for migration analysis

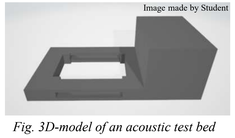
Image made by Student
Fig. 3D-model of an acoustic test bed

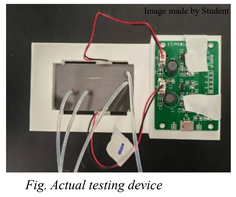
Image made by Student
Fig. Actual testing device

Results

Particle in the Inertial Stage

- Fluorescence microscopy image showing particle motion inside the microfluidic channel under syringe-pump-driven flow.
- Fluorescence image after 2 hours of continuous operation.
- CTC-scale particles are highly enriched in the target outlet.

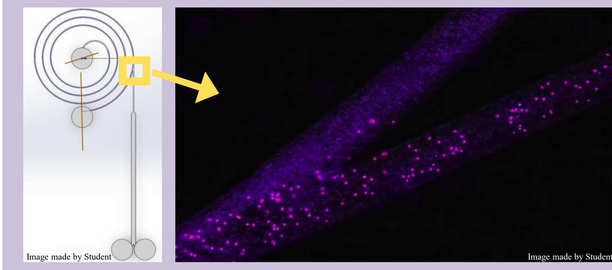
Image made by Student

> 96% CTC enrichment efficiency was achieved based on image-based particle counting

Particle in the Acoustic Stage

- Inertially pre-focused cells enter straight channel with overlapping lateral distribution
- Acoustic OFF: particles remain mixed across channel width
- Acoustic ON: standing wave induces transverse acoustic radiation force Larger CTC analogs migrate faster toward pressure nodes
- Lateral separation becomes evident along channel length
- Spatial segregation enables downstream outlet discrimination

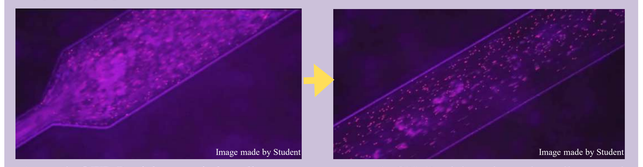
Image made by Student

Acoustic OFF: Particles remain broadly mixed across the channel

Acoustic ON: Particles migrate laterally toward pressure nodes in a size-dependent manner

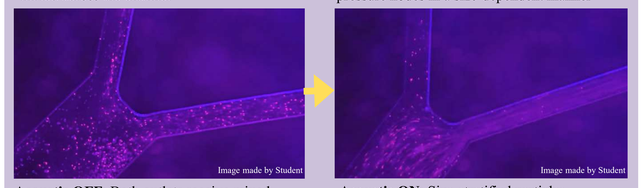
Image made by Student

Acoustic OFF: Both outlets receive mixed particles

Acoustic ON: Size-stratified particles preferentially enter separate outlet branches

Anti-Adhesion

- PS particles exhibited partial wall adhesion during flow
- After Chemical coating was introduced into the suspension

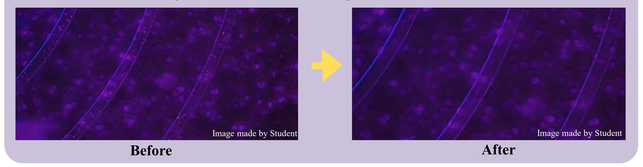
Image made by Student

Before **After**

Conclusion

Novelty

- Dual-field, integrating inertial focusing + acoustic manipulation
- Hybrid anti-adhesion design (micropillars + surface chemistry) for stable operation

Key results

- Inertial separation achieves > 96% CTC enrichment efficiency
- Acoustic separation achieves significant separation results

Future work

- ✓ PZT-driven acoustic separation
- ✓ Integrated lab-on-chip system, combining:
- ✓ syringe-based fluid injection
- ✓ on-chip cleaning / anti-fouling operation
- ✓ integrated microscopy
- ✓ AI-based image analysis and automated cell counting
- ✓ Portable CTC analysis platform

Image made by Student

References:

[1] Ultrasonics, 129 (2023) 106911.
[2] Micromachines, 16 (2025) 66.
[3] Langmuir, 38 (2022) 3775–3784.
[4] J. Med. Biol. Eng., 35 (2015) 143–155.
[5] Microchem. J., 208 (2025) 112570.